



# Winter Braids Lecture Notes

Rinat Kashaev

**Combinatorics of the Teichmüller TQFT**

Vol. 3 (2016), Course n° II, p. 1-16.

<[http://wbln.cedram.org/item?id=WBLN\\_2016\\_\\_3\\_\\_A2\\_0](http://wbln.cedram.org/item?id=WBLN_2016__3__A2_0)>

cedram

*Texte mis en ligne dans le cadre du*  
*Centre de diffusion des revues académiques de mathématiques*  
<http://www.cedram.org/>

## Combinatorics of the Teichmüller TQFT

RINAT KASHAEV

### Abstract

Based on the lectures given by the author at the School on braids and low dimensional topology “Winter Braids VI”, University of Lille I, 22-25 February 2016, we review the combinatorics underlying the Teichmüller TQFT, a new type of three-dimensional TQFT with corners where the vector spaces associated with surfaces are infinite dimensional. The geometrical ingredients and the semi-classical behaviour suggest that this theory is related with hyperbolic geometry in dimension three.

### Contents

|                                       |    |
|---------------------------------------|----|
| Introduction                          | 1  |
| Acknowledgements                      | 2  |
| 1. Triangulations and Pachner moves   | 2  |
| 1.1. Standard topological simplexes   | 2  |
| 1.2. Combinatorial simplexes          | 3  |
| 1.3. Ordered $\Delta$ -triangulations | 3  |
| 1.4. Pachner moves                    | 4  |
| 1.5. Algebraic realisations           | 4  |
| 1.6. The case $d = 3$                 | 5  |
| 1.7. The case $d = 4$                 | 5  |
| 2. H-triangulations                   | 8  |
| 2.1. One vertex H-triangulations      | 8  |
| 3. Shaped triangulations              | 11 |
| 4. Teichmüller TQFT                   | 13 |
| 4.1. Kinematical kernel               | 14 |
| 4.2. Dynamical content                | 14 |
| 4.3. Quasi-classical limit            | 15 |
| References                            | 16 |

### Introduction

The famous theorem of Pachner [9] states that arbitrary triangulations of one and the same piecewise linear (PL) manifold can be related by a finite sequence of elementary moves of finitely many types known as *Pachner or bi-stellar moves* [5]. In analogy with the Reidemeister theorem in knot theory, this result gives a combinatorial framework for constructing invariants of PL-manifolds as well as PL topological quantum field theories (TQFT) with corners, provided one realises the Pachner moves algebraically. In dimension three, a first attempt of

using this scheme has been undertaken in the Regge–Ponzano model [11], where the Pachner moves are realised algebraically in terms of the  $6j$ -symbols within the quantum theory of the angular momentum. Subsequent developments have resulted in the Turaev–Viro TQFT model [13] and its generalisations based on the theory of linear tensor categories [12].

In these notes, following [1, 3, 4], we review the combinatorial data underlying the Teichmüller TQFT which is a new type of three-dimensional TQFT with corners where the vector spaces associated with surfaces are infinite dimensional. The underlying combinatorial structure is given by shaped ordered  $\Delta$ -triangulations, which are closely related with hyperbolic geometry in dimension three. Additionally, the semi-classical behaviour of the Teichmüller TQFT also suggests connections with hyperbolic geometry, allowing one to expect that the Teichmüller TQFT is related to quantum Chern–Simons theory with gauge group  $SL(2, \mathbb{C})$ , the double cover of the group of orientation preserving isometries of the three dimensional hyperbolic space.

The notes are organised as follows. In Section 1, we give definitions of standard and combinatorial simplexes, ordered  $\Delta$ -triangulations, and the Pachner moves. In Section 2, we define the H-triangulations and explain in detail how to construct one vertex H-triangulations for knots in  $S^3$  starting from knot diagrams. In Section 3, we define the shaped triangulations and discuss the angle and gluing equations. In Section 4, we describe the construction of the partition function in Teichmüller TQFT and discuss its asymptotic behaviour in the quasi-classical limit.

## Acknowledgements

This work is supported in part by the Swiss National Science Foundation and the center of excellence grant “Center for quantum geometry of Moduli Spaces” from the Danish National Research Foundation.

## 1. Triangulations and Pachner moves

### 1.1. Standard topological simplexes

Let us denote

$$(1.1) \quad [n] := \{0, 1, \dots, n\}, \quad n \in \mathbb{Z}_{\geq 0}.$$

**Definition 1.** The *standard (topological)  $n$ -simplex* is a topological  $n$ -dimensional ball realised as the subset of  $\mathbb{R}_{\geq 0}^{n+1}$  given by

$$(1.2) \quad \Delta^n = \left\{ (t_0, t_1, \dots, t_n) \in \mathbb{R}_{\geq 0}^{n+1} \mid \sum_{i=0}^n t_i = 1 \right\}.$$

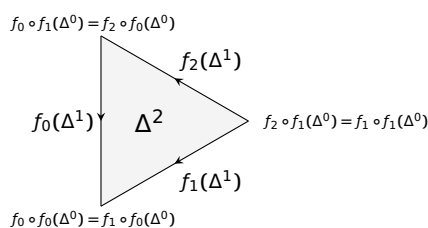
The boundary  $\partial\Delta^n$ , homeomorphic to the  $(n-1)$ -sphere  $S^{n-1}$ , is composed of  $n+1$  homeomorphic images of the standard  $(n-1)$ -simplex through the *face maps*

$$(1.3) \quad f_i: \Delta^{n-1} \rightarrow \Delta^n, \quad (t_0, t_1, \dots, t_{n-1}) \mapsto (t_0, \dots, t_{i-1}, 0, t_i, \dots, t_{n-1}), \quad i \in [n],$$

which satisfy the relations

$$(1.4) \quad f_i \circ f_j = f_{j+1} \circ f_i \quad \text{if } i \leq j.$$

The following picture illustrates the standard 2-simplex:



where the arrows correspond to the standard orientation of the unit interval  $[0, 1] \subset \mathbb{R}$  through the identification

$$(1.5) \quad [0, 1] \rightarrow \Delta^1, \quad t \mapsto (1-t, t).$$

### 1.2. Combinatorial simplexes

**Definition 2.** A *combinatorial  $n$ -simplex*  $\Delta S$  is an abstract simplicial complex given by the power set of a linearly ordered set  $S$  of cardinality  $n + 1$ .

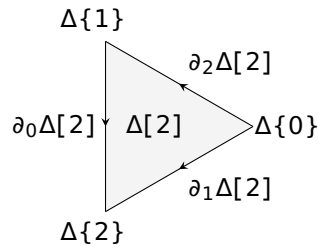
The *standard combinatorial  $n$ -simplex*  $\Delta[n]$  corresponds to the set  $[n] = \{0, 1, \dots, n\}$  with the natural linear order.

It is clear that for any combinatorial  $n$ -simplex  $\Delta S$  there is a unique bijection  $s: [n] \rightarrow S$ ,  $i \mapsto s_i$ , preserving the linear order.

The *facets* or *boundary components* of a combinatorial  $n$ -simplex  $\Delta S$  are combinatorial  $(n-1)$ -simplexes  $\partial_i \Delta S$ ,  $i \in [n]$ , corresponding to the subsets  $S \setminus \{s_i\}$  with the natural induced linear order:

$$(1.6) \quad \partial_i \Delta S = \Delta(S \setminus \{s_i\}).$$

Pictorially, one can still think in terms of the topological simplexes, for example, the combinatorial 2-simplex  $\Delta[2]$  can be drawn as follows



but one should keep in mind that, compared to the face maps (1.3), the operations of taking the boundary components are composed in the opposite order, so that the identity (1.4) should be replaced by

$$(1.7) \quad \partial_j \partial_i = \partial_i \partial_{j+1} \quad \text{if } i \leq j.$$

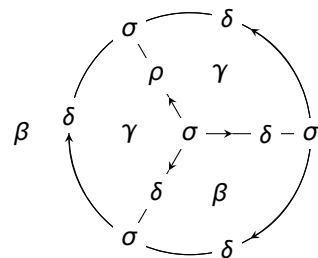
### 1.3. Ordered $\Delta$ -triangulations

**Definition 3.** An *ordered  $\Delta$ -triangulation* is a CW-complex  $X$  where, for any  $n \in \mathbb{Z}_{>0}$ , each  $n$ -cell is given by a characteristic map of the form

$$(1.8) \quad \alpha: \Delta^n \rightarrow X,$$

and, for any  $i \in [n]$ ,  $\alpha \circ f_i$  is the characteristic map of an  $(n-1)$ -cell.

**Example 1.** There exists an ordered  $\Delta$ -triangulation  $X$  of the 3-sphere consisting of one 3-cell, two 2-cells, two 1-cells, and one 0-cell with the following characteristic maps:



$$\begin{aligned} \alpha: \Delta^3 &\rightarrow X, \\ \beta &= \alpha \circ f_0 = \alpha \circ f_3, \\ \gamma &= \alpha \circ f_1 = \alpha \circ f_2, \\ \delta &= \beta \circ f_i = \gamma \circ f_j, \quad i, j \in [2], \quad j \neq 1, \\ \rho &= \gamma \circ f_1, \\ \sigma &= \delta \circ f_i = \rho \circ f_j, \quad i, j \in [1]. \end{aligned}$$

In the picture above, the boundary of the 3-cell is identified with the coordinate plane compactified to a 2-sphere by adding a point at infinity.

In what follows, ordered  $\Delta$ -triangulations will often be informally called just *triangulations*.

### 1.4. Pachner moves

Choose a splitting  $[n] = I \sqcup J$  with non-empty  $I$  and  $J$  of cardinality  $p = |I|$  and  $q = |J|$  so that  $p + q = n + 1$ . The subsets

$$(1.9) \quad \partial_I \Delta^n \equiv \cup_{i \in I} f_i(\Delta^{n-1}) \quad \text{and} \quad \partial_J \Delta^n \equiv \cup_{j \in J} f_j(\Delta^{n-1})$$

are topological  $(n - 1)$ -dimensional balls sharing a common boundary (homeomorphic to the  $(n - 2)$ -sphere  $S^{n-2}$ ). A *Pachner move* of type  $(p, q)$  is the operation of replacing a homeomorphic image of  $\partial_I \Delta^n$  by  $\partial_J \Delta^n$  (a homeomorphic image thereof) in a triangulated  $(n - 1)$ -dimensional manifold.

The Pachner move corresponding to the specific splitting  $[n] = I_0 \sqcup J_0$  with

$$(1.10) \quad I_0 = \left\{ 0, 2, \dots, 2 \left\lfloor \frac{n}{2} \right\rfloor \right\} \quad \text{and} \quad J_0 = \left\{ 1, 3, \dots, 2 \left\lceil \frac{n}{2} \right\rceil - 1 \right\}$$

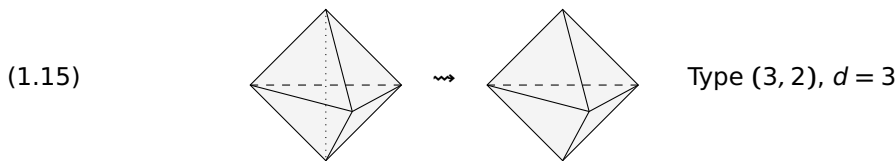
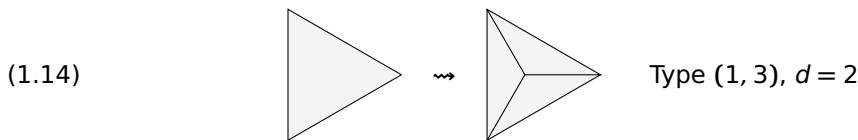
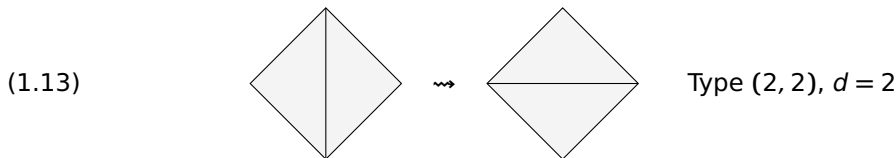
will be called the *distinguished Pachner move*. Here we use the floor  $\lfloor x \rfloor$  (the largest integer not greater than  $x$ ) and the ceiling  $\lceil x \rceil$  (the smallest integer not less than  $x$ ) functions. The corresponding partition of  $n + 1$  is given by the formula

$$(1.11) \quad (p_0, q_0) = (|I_0|, |J_0|) = \left( \left\lfloor \frac{n}{2} \right\rfloor + 1, \left\lceil \frac{n}{2} \right\rceil \right).$$

The following table gives the values for small  $n = d + 1$ :

$$(1.12) \quad \begin{array}{c|ccccccc} d & 1 & 2 & 3 & 4 & 5 & 6 & 7 \\ \hline (p_0, q_0) & (2, 1) & (2, 2) & (3, 2) & (3, 3) & (4, 3) & (4, 4) & (5, 4) \end{array}$$

The following pictures illustrate few Pachner moves in small dimensions.



Pachner's theorem [9], which states that two triangulated PL-manifolds are PL-homeomorphic if and only if they are related by a finite sequence of Pachner moves, allows to construct PL-invariants provided one finds algebraic realisations of the Pachner moves. A typical example are the Turaev–Viro invariants of 3-manifolds [13] which are based on the theory of 6j-symbols of the representation theory of Hopf algebras giving algebraic realisations of the Pachner moves of the types  $(p, 5 - p)$ ,  $p \in \{1, 2, 3, 4\}$ , which are closely related to *Matveev–Piergallini moves* in the dual language of special spines of 3-manifolds [6, 7, 10].

### 1.5. Algebraic realisations

A restricted class of algebraic realisations of the Pachner moves in  $d$  dimensions can be obtained as follows.

One associates a (finite dimensional) complex vector space  $V(s)$  to each  $(d - 1)$ -simplex  $s$ , and a vector  $V(p) \in V(\partial_0 p) \otimes \dots \otimes V(\partial_d p)$  to each  $d$ -simplex  $p$  in such a way that if  $s^*$

is a  $(d - 1)$ -simplex  $s$  with opposite (induced) orientation then the associated vector space should be the dual vector space  $V(s)^* = V(s^*)$ , and the functorial properties with respect to the gluing operations should be satisfied. In particular, for the distinguished Pachner moves, the following equality should be satisfied:

$$(1.16) \quad (\otimes_{k < l} \text{Ev}_{2k,2l})(\otimes_i V(\partial_{2i}u)) = (\otimes_{k < l} \text{Ev}_{2k+1,2l+1})(\otimes_j V(\partial_{2j+1}u))$$

where  $u$  is a  $(d + 1)$ -simplex and

$$(1.17) \quad \text{Ev}_{i,j}: V(\partial_i \partial_j u)^* \otimes V(\partial_i \partial_j u) \rightarrow \mathbb{C}$$

is the operation of contracting between elements of dual vectors spaces. In this way, one arrives at a multilinear algebraic relation on the vectors associated to the  $d$ -simplexes. The following table gives a list of algebraic structures which can be used for realisation of at least the distinguished Pachner moves in dimensions up to 3:

| $d$                 | 1          | 2        | 3           |
|---------------------|------------|----------|-------------|
| algebraic structure | projectors | algebras | bi-algebras |

### 1.6. The case $d = 3$

The distinguished Pachner move of the type  $(3, 2)$  can be realised by a linear map  $S: V \otimes V \rightarrow V \otimes V$  satisfying the equality

$$(1.18) \quad S_{1,2} S_{1,3} S_{2,3} = S_{2,3} S_{1,2}$$

where  $V$  is a vector space and  $S_{i,j}$  is an element of the endomorphism algebra of the vector space  $V^{\otimes 3}$  acting as  $S$  in the  $i$ -th and  $j$ -th components and identically in the remaining component, e.g.  $S_{1,2} = S \otimes \text{id}_V$ . Namely, for any oriented 2-simplex (triangle)  $t$  we assign the vector space  $V(t) = V$  and for any oriented 3-simplex (tetrahedron)  $s$  the vector

$$(1.19) \quad V(s) = S \in V(\partial_0 s) \otimes V(\partial_1 s) \otimes V(\partial_2 s) \otimes V(\partial_3 s) = V \otimes V^* \otimes V \otimes V^* = \text{End}(V \otimes V)$$

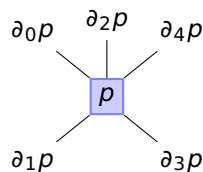
where we use the fact that the induced orientations on the even facets of a simplex are opposite to those on the odd facets. If  $V$  is provided with the structure of a bi-algebra with the multiplication  $\nabla_V: V \otimes V \rightarrow V$  and the co-multiplication  $\Delta_V: V \rightarrow V \otimes V$ , then the element

$$(1.20) \quad S = (\text{id}_V \otimes \nabla_V)(\Delta_V \otimes \text{id}_V): V \otimes V \rightarrow V \otimes V$$

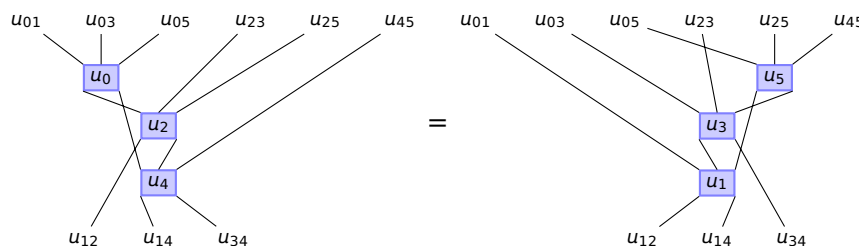
is easily seen to satisfy relation (1.18).

### 1.7. The case $d = 4$

Let  $p$  be an oriented 4-simplex also called *pentachoron*. We will find it convenient to represent a pentachoron diagrammatically as a five valent vertex



which allows to represent the distinguished Pachner move of the type  $(3, 3)$  as the following (string) diagrammatic equality



where  $u$  is a 5-simplex with the notation

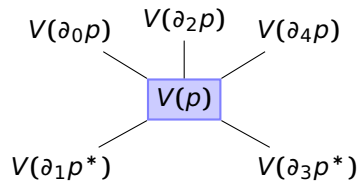
$$u_i \equiv \partial_i u, \quad u_{ij} \equiv \partial_i \partial_j u,$$

and the internal edges correspond to internal shared tetrahedra. Specifically, the internal edge connecting the pentachora  $u_i$  and  $u_j$  with  $i < j$  correspond to the common internal tetrahedron  $u_{ij}$  shared between those pentachora.

Using the fact that the induced orientations on even facets are opposite to those on odd facets, the vector  $V(p) \in V(\partial_0 p) \otimes \cdots \otimes V(\partial_4 p)$  can be thought of as a linear map

$$V(p): V(\partial_1 p^*) \otimes V(\partial_3 p^*) \rightarrow V(\partial_0 p) \otimes V(\partial_2 p) \otimes V(\partial_4 p)$$

with a similar string diagrammatic notation as for an abstract pentachoron



In the simplest case of a constant realisation

$$(1.21) \quad V(p) = Q \equiv \begin{array}{c} \diagup \\ \square Q \\ \diagdown \end{array} : V \otimes V \rightarrow V \otimes V \otimes V$$

we arrive at a graphical equation to be called *Pachner (3,3)-relation*

$$(1.22) \quad \begin{array}{c} \diagup \\ \square Q \\ \diagdown \end{array} \begin{array}{c} \diagup \\ \square Q \\ \diagdown \end{array} \begin{array}{c} \diagup \\ \square Q \\ \diagdown \end{array} = \begin{array}{c} \diagup \\ \square Q \\ \diagdown \end{array} \begin{array}{c} \diagup \\ \square Q \\ \diagdown \end{array} \begin{array}{c} \diagup \\ \square Q \\ \diagdown \end{array}$$

whose analytic form reads as

$$(1.23) \quad (Q\sigma \otimes \text{id}_{V^{\otimes 3}})(\text{id}_V \otimes Q \otimes \text{id}_V)(\sigma \otimes \text{id}_{V^{\otimes 2}})(\text{id}_V \otimes Q) \\ = (\text{id}_{V^{\otimes 2}} \otimes \sigma \otimes \text{id}_{V^{\otimes 2}})(\text{id}_{V^{\otimes 3}} \otimes Q\sigma)(\text{id}_V \otimes Q \otimes \text{id}_V)(\text{id}_{V^{\otimes 2}} \otimes \sigma)(Q \otimes \text{id}_V)$$

where  $\sigma = \sigma_{V,V}$  is the permutation operator defined by

$$(1.24) \quad \sigma_{X,Y}: X \otimes Y \rightarrow Y \otimes X, \quad x \otimes y \mapsto y \otimes x, \quad \forall x \in X, \forall y \in Y.$$

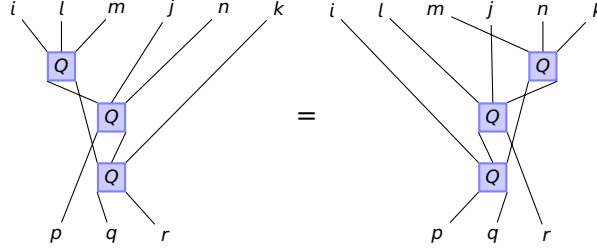
We can also use the same graphical notation

$$Q_{l,m}^{i,j,k} \equiv \begin{array}{c} i \quad j \quad k \\ \diagup \\ \square Q \\ \diagdown \\ l \quad m \end{array} \in \mathbb{C}$$

for the *matrix coefficients*

$$Q_{l,m}^{i,j,k} \equiv \langle Q, \omega^i \otimes e_l \otimes \omega^j \otimes e_m \otimes \omega^k \rangle = \langle \omega^i \otimes \omega^j \otimes \omega^k, Q(e_l \otimes e_m) \rangle$$

associated with dual linear bases  $\{e_i\} \subset V$  and  $\{\omega^j\} \subset V^*$ . In this way, we obtain a coordinate form of the Pachner (3,3)-relation given by a system of non-linear algebraic equations



where summations over the implicit indices on the internal edges are assumed. The explicit analytic form of these equations reads as follows:

$$(1.25) \quad \sum_{s,t,u} Q_{s,t}^{i,l,m} Q_{p,u}^{s,j,n} Q_{q,r}^{t,u,k} = \sum_{s,t,u} Q_{s,t}^{m,n,k} Q_{u,r}^{l,j,t} Q_{p,q}^{i,u,s}.$$

**Example 2.** For any abelian group  $A$  and a bi-character  $\chi: A \times A \rightarrow \mathbb{C}$ , we have a solution in the form of a linear operator between the vector spaces of complex valued functions on  $A^2$  and  $A^3$ :

$$(1.26) \quad Q: \mathbb{C}^{A^2} \rightarrow \mathbb{C}^{A^3}, \quad (Qf)(x, y, z) = \chi(x, z)f(x + y, y + z).$$

If  $A$  is a locally compact abelian (abbreviated as LCA) group, then the matrix coefficients make sense as tempered distributions over  $A^5$ :

$$(1.27) \quad Q_{u,v}^{x,y,z} = D\chi(x, u, y, v, z) := \chi(x, z)\delta(x - u + y)\delta(y - v + z), \quad \forall(x, y, z, u, v) \in A^5,$$

where  $\delta(x)$  is Dirac's delta distribution over  $A$  defined by

$$(1.28) \quad \int_A \delta(x)f(x) dx = f(0)$$

with a chosen Haar measure  $dx$  on  $A$  and any Schwartz–Bruhat test function  $f: A \rightarrow \mathbb{C}$ . Equations (1.25) are satisfied by (1.27), provided the summations are interpreted as integrations with respect to the Haar measure. Indeed, for any  $(i, j, k, l, m, n, p, q, r) \in A^9$ , we have two tempered distributions

$$(1.29) \quad \begin{aligned} & \int_{A^3} Q_{s,t}^{i,l,m} Q_{p,u}^{s,j,n} Q_{q,r}^{t,u,k} d(s, t, u) \\ &= \int_{A^3} \chi(i, m)\delta(i - s + l)\delta(l - t + m)Q_{p,u}^{s,j,n} Q_{q,r}^{t,u,k} d(s, t, u) \\ &= \chi(i, m) \int_A Q_{p,u}^{i+l,j,n} Q_{q,r}^{l+m,u,k} du \\ &= \chi(i, m) \int_A \chi(i + l, n)\delta(i + l - p + j)\delta(j - u + n)Q_{q,r}^{l+m,u,k} du \\ &= \chi(i, m)\chi(i + l, n)\delta(i + l - p + j)Q_{q,r}^{l+m,j+n,k} \\ &= \chi(i, m)\chi(i + l, n)\chi(l + m, k)\delta(i + l - p + j)\delta(l + m - q + j + n)\delta(j + n - r + k) \end{aligned}$$



and

$$\begin{aligned}
 (1.30) \quad & \int_{A^3} Q_{s,t}^{m,n,k} Q_{u,r}^{l,j,t} Q_{p,q}^{i,u,s} d(s, t, u) \\
 &= \int_{A^3} \chi(m, k) \delta(m-s+n) \delta(n-t+k) Q_{u,r}^{l,j,t} Q_{p,q}^{i,u,s} d(s, t, u) \\
 &= \chi(m, k) \int_A Q_{u,r}^{l,j,n+k} Q_{p,q}^{i,u,m+n} du \\
 &= \chi(m, k) \int_A \chi(l, n+k) \delta(l-u+j) \delta(j-r+n+k) Q_{p,q}^{i,u,m+n} du \\
 &= \chi(m, k) \chi(l, n+k) \delta(j-r+n+k) Q_{p,q}^{i,l+j,m+n} \\
 &= \chi(m, k) \chi(l, n+k) \chi(i, m+n) \delta(j-r+n+k) \delta(i-p+l+j) \delta(l+j-q+m+n)
 \end{aligned}$$

which coincide due to the fact that  $\chi(x, y)$  is a bi-character.

## 2. H-triangulations

**Definition 4.** An *H-triangulation* is a pair  $(X, H)$  where  $X$  is an ordered  $\Delta$ -triangulation of a closed compact oriented 3-manifold and  $H$  is a vertex-disjoint simple cycle cover of the 1-skeleton of  $X^1$ .

The Pachner moves in 3 dimensions have natural relative versions adapted to H-triangulations, and the corresponding equivalence classes are in bijection with the topological classes of pairs  $(M, L)$  where  $M$  is a closed compact oriented 3-manifold and  $L \subset M$  is a link [2].

### 2.1. One vertex H-triangulations

Let  $(M, K)$  be a pair consisting of a closed compact oriented 3-manifold  $M$  and a knot  $K \subset M$ . A one vertex H-triangulation of  $(M, K)$  is a triangulation of  $M$  with one vertex and a distinguished edge representing the knot  $K$ . A one vertex H-triangulation of a knot in  $S^3$  can be constructed starting from a non-trivial knot diagram  $D$  as follows.

First, take  $S^3$  as the standard one point compactification of  $\mathbb{R}^3$  and fix an embedding  $S^2 \subset S^3$  as the closure of the standard embedding  $\mathbb{R}^2 \subset \mathbb{R}^3$ ,  $(x, y) \mapsto (x, y, 0)$ . Next, we choose  $D$  as the image of a polygonal knot  $K \subset \mathbb{R}^2 \times [-\epsilon, \epsilon] \subset \mathbb{R}^3$  under the orthogonal projection of  $\mathbb{R}^3 \rightarrow \mathbb{R}^2$ , with a small positive real  $\epsilon$ , so that the vertices of  $K$  project to mid-points of the edges of  $D$  (here we think of  $D$  as a 4-valent graph with vertices at crossings), except for one distinguished edge, to which we assume two vertices of  $K$  are projected. We consider  $K$  together with its natural cellular decomposition. In the case of the figure-eight knot, the diagram in Fig. 2.1(a) satisfies all these conditions where the images of the vertices of the cellular decomposition of  $K$  are represented by small filled circles and the distinguished edge of  $D$  is the one containing the uppermost horizontal segment.

The cellular decomposition of  $K$  extends to that of  $S^3$  by keeping the same vertex set and adding new edges so that each crossing point of  $D$  is surrounded by the images of four new edges as in Fig. 2.1(b) where the higher dimensional cells are given by tetrahedral cells contained in  $\mathbb{R}^2 \times [-\epsilon, \epsilon]$ , together with their own natural cellular structure and which are projected to shaded quadrilaterals containing the crossings of  $D$  and also by two 3-cells  $\tilde{c}_\pm$  given by the intersections of the complements of the tetrahedral cells in  $S^3$  with the two balls  $B_+$  and  $B_-$  obtained as closures in  $S^3$  of the upper and lower half spaces respectively, i.e.

$$(2.1) \quad B_\pm = \overline{\{(x, y, z) \in \mathbb{R}^3 \cup \{\infty\} \mid \pm z \geq 0\}}$$

so that  $S^3 = B_+ \cup B_-$  and  $S^2 = B_+ \cap B_-$ .

<sup>1</sup>Here we use the graph theoretical terminology, where, for a given graph, a *vertex-disjoint simple cycle cover* is a subgraph containing all the vertices of the graph and which topologically is a disjoint union of circles.

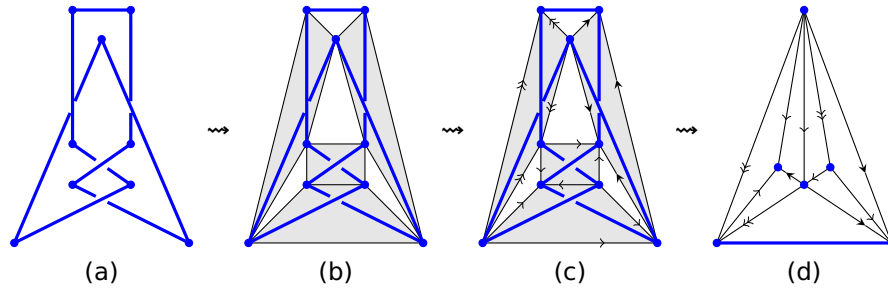


Figure 2.1: Construction of a one vertex cell decomposition of the pair  $(S^3, 4_1)$ : (a) a knot diagram with a cellular structure; (b) the induced cellular decomposition of  $S^3$  with crossings contained in shaded tetrahedral cells; (c) each shaded tetrahedron is collapsed to a segment represented by four oriented edges of the tetrahedron; (d) the result of gluing of the cells  $c_{\pm}$  along the 2-cell corresponding to the outer region of the knot diagram.

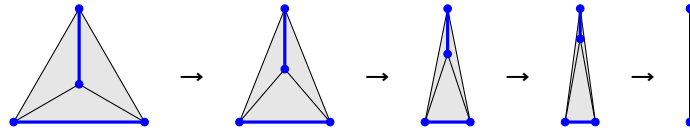


Figure 2.2: An isotopy which collapses a tetrahedron to a segment.

From the constructed cellular decomposition of  $S^3$  we produce a new cellular complex by an isotopy which starts from the identity map and ends with a projection to a topological quotient space (still homeomorphic to  $S^3$ ) with respect to the equivalence relation under which all points of  $K$ , except the segment which projects to the distinguished edge of  $D$ , are equivalent to each other, and each tetrahedral cell is collapsed to a single edge as in Fig. 2.2. The resulting cellular complex is composed of two 3-cells  $c_{\pm}$ , the images of  $\tilde{c}_{\pm}$ , while the 2-skeleton is given by the complementary regions of the quadrilaterals containing the crossings of the diagram  $D$  as in Fig. 2.1(c) where the non-collapsed part of  $K$  is the uppermost horizontal segment, and the 2-cells are given by non-shaded regions, namely four triangular cells and one quadrilateral cell corresponding to the outer region. The orientations on the edges with different types of arrows allow to keep track of the information on their identifications, namely, one type of arrow corresponds to one and the same (geometrical) edge, the image of the corresponding collapsed tetrahedron.

By gluing two 3-cells  $c_{\pm}$  together along the 2-cell corresponding to the outer region in the knot diagram we obtain a cellular complex given by one 3-cell whose boundary is composed of the remaining 2-cells, each 2-cell appearing twice with opposite orientations as in Fig. 2.1(d) where the boundary 2-sphere of the 3-cell is identified with the coordinate plane compactified to a 2-sphere by adding a point at infinity. The obtained complex can be non-canonically transformed into a  $\Delta$ -triangulation by cutting the 3-cell into tetrahedra. In our example this is achieved by cutting along two new triangular 2-cells, see Fig. 2.3(b), where a linear order of vertices of each tetrahedron is induced by the directions of arrows on the edges.

Below, we present three more examples of one vertex H-triangulations of the knots  $3_1$ ,  $5_2$  and  $6_1$  in  $S^3$ .

**Example 3** (One vertex H-triangulation of  $(S^3, 3_1)$ ). The construction is given by Fig. 2.4. Namely, as explained in Subsection 2.1, the diagram (a) of the trefoil knot induces a cellular decomposition (b) of  $S^3$  which, upon removing the 2-cell corresponding to the outer region of

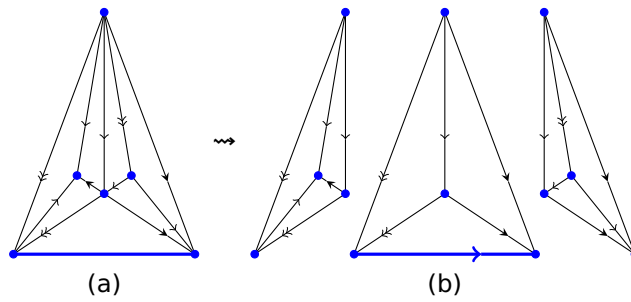


Figure 2.3: A one-vertex H-triangulation of the pair  $(S^3, 4_1)$  with three tetrahedra.

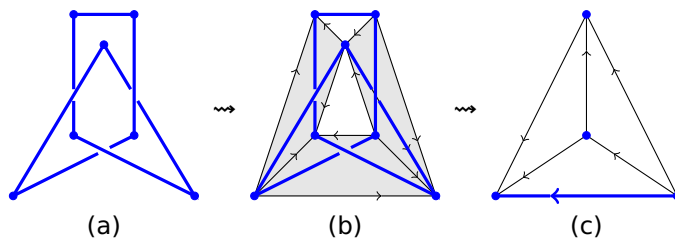


Figure 2.4: Construction of a one vertex H-triangulation of the pair  $(S^3, 3_1)$ .

(b), immediately gives rise to H-triangulation (c). Thus, we have one tetrahedron  $T$  with the face identifications

$$(2.2) \quad \partial_i T \sim \partial_{3-i} T, \quad i \in \{0, 1\}.$$

The quotient space  $X$  is a triangulation of  $S^3$  with one vertex and two edges: the edge  $\bullet \rightarrow \bullet$  in Fig. 2.4(c), which is knotted like trefoil and has the only edge  $03$  of  $T$  as pre-image and the edge  $\bullet \rightarrow \bullet$  in Fig. 2.4(c), having all five other edges of  $T$  as pre-images. The obtained triangulation is, in fact, the one described in Example 1.

**Example 4** (One vertex H-triangulation of  $(S^3, 5_2)$ ). The construction is given in Fig. 2.5 where in the last picture (d) one can easily identify four tetrahedra piled up from bottom to

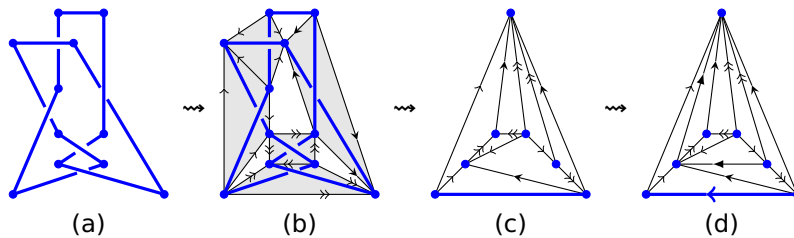


Figure 2.5: Construction of a one vertex H-triangulation of the pair  $(S^3, 5_2)$ .

top. Enumerating them as  $T_i, i \in [3]$ , in the order from bottom to top, we have the following

face identifications:

$$(2.3) \quad \partial_2 T_0 \sim \partial_3 T_0, \partial_0 T_0 \sim \partial_3 T_2, \partial_1 T_0 \sim \partial_0 T_1, \partial_1 T_1 \sim \partial_0 T_2, \\ \partial_2 T_1 \sim \partial_1 T_3, \partial_3 T_1 \sim \partial_0 T_3, \partial_1 T_2 \sim \partial_2 T_3, \partial_2 T_2 \sim \partial_3 T_3.$$

**Example 5** (One vertex H-triangulation of  $(S^3, 6_1)$ ). The construction is given in Fig. 2.6 where in the last picture (d) one can easily identify five tetrahedra piled up from bottom to top. Enumerating them as  $T_i, i \in [4]$ , in the order from bottom to top, we have the following face identifications:

$$(2.4) \quad \partial_2 T_0 \sim \partial_3 T_0, \partial_0 T_0 \sim \partial_0 T_1, \partial_1 T_0 \sim \partial_3 T_3, \partial_1 T_1 \sim \partial_2 T_2, \partial_2 T_1 \sim \partial_0 T_4, \\ \partial_3 T_1 \sim \partial_0 T_2, \partial_1 T_2 \sim \partial_1 T_4, \partial_3 T_2 \sim \partial_0 T_3, \partial_1 T_3 \sim \partial_3 T_4, \partial_2 T_3 \sim \partial_2 T_4.$$

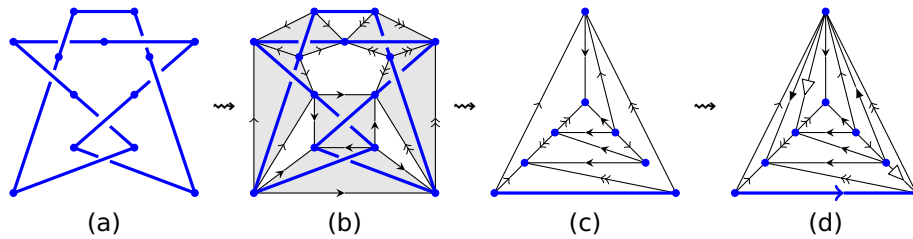
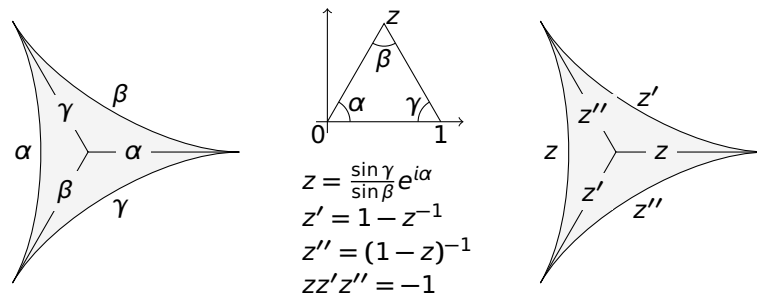


Figure 2.6: Construction of a one vertex H-triangulation of the pair  $(S^3, 6_1)$ .

### 3. Shaped triangulations

**Definition 5.** A triangulation  $X$  is called *shaped* if each tetrahedron of  $X$  carries the structure of an ideal hyperbolic tetrahedron.

The shape of one tetrahedron can be described either by dihedral angles or by complex shape variables associated with edges according to the following rules:



**Definition 6.** Let  $X$  be a shaped triangulation. The (*complex*) *weight*  $w(e)$  of edge  $e$  of  $X$  is the product of all tetrahedral shapes associated with this edge. The *total angle*  $\alpha(e)$  at edge  $e$  of  $X$  is the sum of all dihedral angles around that edge.

We have the following evident formula

$$(3.1) \quad w(e) = |w(e)|e^{i\alpha(e)}.$$

**Definition 7.** An edge  $e$  of a triangulation  $X$  is called *weight* (respectively *angle*) *balanced* if its weight (respectively the total angle) is equal to 1 (respectively  $2\pi$ ).

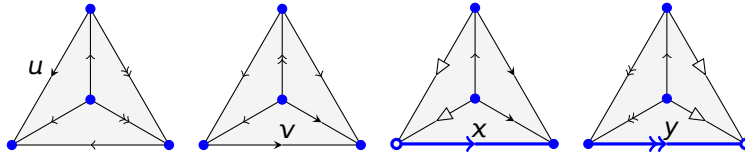
(Thurston's) gluing equations (respectively angle (structure) equations) of a triangulation  $X$  of a cusped 3-manifold correspond to weight (respectively angle) balancing of all edges of  $X$ .

**Remark 1.** For any shaped triangulation, define its volume as the sum of volumes of all tetrahedra. Then, maximisation of the volume in the space of angle structures corresponds to completing the angle equations to gluing equations together with the completeness condition. More generally, maximisation of the volume in the subspace of all shape structures with fixed total angles around edges corresponds to identification of the complete hyperbolic structure with the cone singularities specified by the total angles.

**Remark 2.** The gluing (respectively angle) equations are compatible with the Pachner moves of the type (3,2) provided the edge associated to the move is weight (respectively angle) balanced. In that case, the move will be called *shaped* (respectively *angled*).

The last remark allows us to impose the gluing or angle equations only partially and to consider them in the broader context of arbitrary triangulations. As one cannot apply the (3,2) Pachner move along the non-balanced edges, the latter should be considered as an additional structure of the underlying 3-manifold or topological space.

**Example 6.** Consider the following 2-vertex H-triangulation of the pair  $(S^3, 4_1)$ :



where the knot is represented by the bottom edges of the last two tetrahedra, and we indicate the complex shape variables next to their associated edges. The edge weights are as follows:

$$(3.2) \quad w(\circ \rightarrow \bullet) = x, \quad w(\bullet \rightarrow \circ) = y,$$

$$(3.3) \quad w(\bullet \rightarrow \bullet) = x'x''y'y'' = \frac{1}{xy},$$

$$(3.4) \quad w(\bullet \rightarrow \bullet) = uvv'x'x'' = \frac{u}{v''x'},$$

$$(3.5) \quad w(\bullet \rightarrow \bullet) = uu'vy'y'' = \frac{v}{u''y'},$$

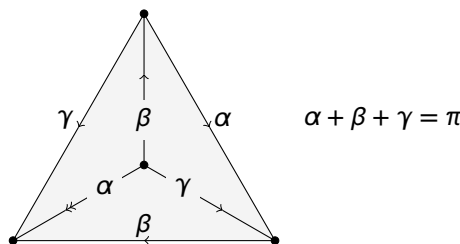
$$(3.6) \quad w(\bullet \rightarrow \bullet) = u'(u'')^2v'(v'')^2xy = \frac{u''v''xy}{uv}.$$

Imposing the gluing equations on all edges except those representing the knot, we obtain

$$(3.7) \quad xy = 1, \quad (1 - v)u = x, \quad (1 - u)v = y.$$

We observe that system (3.7) describes the deformation variety of the figure-eight knot complement, where the variables  $x$  and  $y$  are naturally associated with the meridian. In particular, the additional condition  $x = y = 1$  in (3.7) corresponds to the complete hyperbolic structure.

**Example 7.** Let  $X$  be the one tetrahedron triangulation of  $S^3$  from Example 1. Taking a shape structure on  $X$  given by dihedral angles  $\alpha, \beta, \gamma$  according to this picture



we obtain the following total angles:

$$(3.8) \quad \alpha(\bullet \dashrightarrow \bullet) = \alpha, \quad \alpha(\bullet \rightarrow \bullet) = \alpha + 2\beta + 2\gamma = 2\pi - \alpha$$

which depend only on the angle  $\alpha$ , but not on  $\beta$  or  $\gamma$ . Geometrically, the total angles determine a (hyperbolic) metric with conical singularities along the unbalanced edges. Maximisation of the volume of  $X$  with fixed conical singularities (i.e. fixed  $\alpha$ ) fixes the angles  $\beta$  and  $\gamma$  in terms of  $\alpha$ . Indeed, the volume of an ideal hyperbolic tetrahedron with dihedral angles  $\alpha, \beta, \gamma$  is given by Milnor's formula [8]

$$(3.9) \quad \text{vol}(\alpha, \beta, \gamma) = \Lambda(\alpha) + \Lambda(\beta) + \Lambda(\gamma),$$

where

$$(3.10) \quad \Lambda(x) := - \int_0^x \log |2 \sin \theta| d\theta$$

is Lobachevsky's function which is antisymmetric

$$(3.11) \quad \Lambda(-x) = -\Lambda(x)$$

and  $\pi$ -periodic

$$(3.12) \quad \Lambda(x + \pi) = \Lambda(x).$$

The critical points of  $\text{vol}(\alpha, \beta, \gamma)$  at fixed  $\alpha$  are given by the equations

$$(3.13) \quad d \text{vol}(\alpha, \beta, \gamma)|_{d\alpha=0} = 0 \iff \Lambda'(\beta) = \Lambda'(\gamma) \iff \beta = \gamma = \frac{\pi - \alpha}{2},$$

so that the volume of the complete hyperbolic structure on  $X$  with conical singularities along its 1-skeleton determined by  $\alpha$  is given by the formula

$$(3.14) \quad \text{vol}(X) = \text{vol}(\alpha, \beta, \gamma)|_{\beta=\gamma} = 2\Lambda(\alpha/2),$$

where we have used the formula

$$(3.15) \quad \Lambda(2x) = 2\Lambda(x) + 2\Lambda\left(x + \frac{\pi}{2}\right).$$

In the next section, we obtain this result by taking the quasi-classical limit of the Teichmüller TQFT partition function of  $X$ , which, due to the gauge invariance in the space of shape structures, depends also only on the angle  $\alpha$  but not on  $\beta$  or  $\gamma$ .

#### 4. Teichmüller TQFT

For two sets  $A$  and  $B$  we will denote by  $A^B$  the set of maps from  $B$  to  $A$ . For any finite set  $E$  we denote by  $\mathcal{S}(\mathbb{R}^E)$  the set of Schwartz class functions on  $\mathbb{R}^E$  and by  $\mathcal{S}'(\mathbb{R}^E)$  the dual space of tempered distributions on  $\mathbb{R}^E$ . We will also denote by  $X_i$  the set of  $i$ -simplexes of a triangulation  $X$ . In a triangulation of an oriented pseudo 3-manifold, there two types of tetrahedra:



where the linear order on the vertices is given by the number of incoming arrows. We will denote by  $\varepsilon(T) \in \{\pm 1\}$  the sign of tetrahedron  $T$ .

#### 4.1. Kinematical kernel

Let  $X$  be a triangulation. Define a map

$$(4.1) \quad \rho: X_3 \rightarrow S'(\mathbb{R}^{X_2} \times \mathbb{R}^{X_3}),$$

$$\rho(T)(x, y) = e^{2\pi i \varepsilon(T) x_0 y(T)} \delta(x_0 - x_1 + x_2) \delta(x_2 - x_3 + y(T)), \quad x_i := x(\partial_i T).$$

**Remark 3.** Formula (4.1) can also be written in terms of the distribution valued solution (1.27) of the Pachner (3, 3)-relation (1.25) in the case of the LCA group  $\mathbb{R}$ :

$$(4.2) \quad \rho(T)(x, y) = D_\chi(x_0, x_1, x_2, x_3, y(T))$$

where the bi-character  $\chi$  is given by the formula

$$(4.3) \quad \chi(s, t) = e^{2\pi i \varepsilon(T) s t}, \quad \forall (s, t) \in \mathbb{R}^2.$$

**Definition-Proposition 1.** Let  $X$  be a triangulation of a compact closed oriented pseudo 3-manifold satisfying the condition  $H^2(X \setminus X_0, \mathbb{Z}) = 0$ . The kinematical kernel of  $X$  is an element  $K_X \in S'(\mathbb{R}^{X_3})$  defined by the integral

$$(4.4) \quad K_X(y) = \int_{\mathbb{R}^{X_2}} dx \prod_{T \in X_3} \rho(T)(x, y).$$

We do not give the proof here, but it is an implicit part of the proof of Theorem 7 of [1] as it will be clear from equality (4.17) in the next subsection.

**Example 8.** Let  $X$  be the triangulation from Example 1. We have

$$(4.5) \quad X_3 = \{T\}, \quad X_2 = \{F_1, F_2\}, \quad (\partial_i T)_{i=0}^3 = (F_1, F_2, F_2, F_1), \quad \varepsilon(T) = 1$$

so that

$$(4.6) \quad \rho(T)(x, y) = e^{2\pi i x_1 y} \delta(x_1 - x_2 + x_2) \delta(x_2 - x_1 + y)$$

$$= \delta(x_1) \delta(x_2 + y), \quad x_i := x(F_i), \quad y := y(T)$$

and thus

$$(4.7) \quad K_X(y) = \int_{\mathbb{R}^2} d(x_1, x_2) \delta(x_1) \delta(x_2 + y) = 1.$$

#### 4.2. Dynamical content

We fix a positive real parameter  $\hbar$ , and we let  $b$  denote a solution of the equation

$$(4.8) \quad (b + b^{-1})\sqrt{\hbar} = 1$$

satisfying the inequalities

$$(4.9) \quad \Re b > 0, \quad \Im b \geq 0.$$

We also denote

$$(4.10) \quad \vartheta := \frac{b + b^{-1}}{2\pi} = \frac{1}{2\pi\sqrt{\hbar}}.$$

Let  $X$  be a shaped triangulation. We define a map

$$(4.11) \quad \psi: X_3 \rightarrow \mathbb{C}^{\mathbb{R}^{X_3}}, \quad \psi(T)(y) = \frac{e^{2\pi \vartheta \alpha_3 y(T)}}{\Phi_b(y(T) - i\vartheta \varepsilon(T)(\alpha_2 + \alpha_3))^{\varepsilon(T)}}$$

where

$$(4.12) \quad \alpha_i := \text{angle}(\partial_0 \partial_i T), \quad \forall i \in \{1, 2, 3\},$$

and

$$(4.13) \quad \Phi_b(x) := \exp\left(\frac{1}{4} \int_{\mathbb{R}+i0} \frac{e^{-2ixz}}{\sinh(bz) \sinh(b^{-1}z)} \frac{dz}{z}\right)$$

is Faddeev's quantum dilogarithm which is a meromorphic function on the entire complex plane with the zeros and poles located outside the strip

$$(4.14) \quad |\Im x| < \pi \vartheta$$

and satisfying the unitarity condition under the complex conjugation

$$(4.15) \quad \overline{\Phi_b(x)} = \frac{1}{\Phi_b(\bar{x})}.$$

**Definition-Proposition 2.** Let  $X$  be a shaped triangulation. The dynamical content of  $X$  is a test function  $D_X \in \mathcal{S}(\mathbb{R}^{X_3})$  defined by the following product formula:

$$(4.16) \quad D_X(y) = \prod_{T \in X_3} \psi(T)(y).$$

The fact that  $D_X \in \mathcal{S}(\mathbb{R}^{X_3})$  is a consequence of the properties of Faddeev's quantum dilogarithm and the positivity of the dihedral angles, see for details [1].

**Theorem 1.** Let  $X$  be a shaped triangulation of a compact closed oriented pseudo 3-manifold  $M$  satisfying the condition  $H^2(X \setminus X_0, \mathbb{Z}) = 0$ . Then the absolute value of the Teichmüller TQFT partition function defined by

$$(4.17) \quad Z_{\hbar}(X) = K_X(D_X) = \int_{\mathbb{R}^{X_3}} K_X(y) D_X(y) dy$$

is invariant under angled (3, 2) Pachner moves. If additionally  $M$  is a manifold (i.e. without cusps) then  $|Z_{\hbar}(X)|$  depends only on the total dihedral angles.

This theorem follows from Theorem 4 of [1]. Its last part is a consequence of the gauge invariance in the space of shape structures induced by the Hamiltonian action of the group  $\mathbb{R}^{|X_1|-1}$  through the Neumann–Zagier Poisson structure and where the Hamiltonians are given by the total angles.

**Example 9.** Let  $X$  be the triangulation from Example 1, see also Examples 7 and 8 for notation. We have

$$(4.18) \quad K_X(y) = 1, \quad D_X(y) = \frac{e^{2\pi\vartheta\alpha y}}{\Phi_b(y - i\vartheta(\alpha + \gamma))}$$

so that

$$(4.19) \quad |Z_{\hbar}(X)| = \left| \int_{\mathbb{R}} \frac{e^{2\pi\vartheta\alpha y}}{\Phi_b(y - i\vartheta(\alpha + \gamma))} dy \right| = \left| \int_{\mathbb{R} - i\vartheta(\alpha + \gamma)} \frac{e^{2\pi\vartheta\alpha z}}{\Phi_b(z)} dz \right| = |\Phi_b(i\vartheta(\pi - \alpha))|$$

where in the last equality we have used the Fourier transformation formula of Faddeev's quantum dilogarithm:

$$(4.20) \quad \int_{\mathbb{R} + i\epsilon} \Phi_b(y) e^{2\pi i x y} dy = \zeta_0 e^{-\pi i x^2} \Phi_b(x + i\pi\vartheta), \quad 0 < -\Im x < \epsilon < \pi\vartheta, \quad \zeta_0 := e^{\pi i(1+\hbar^{-1})/12}.$$

From the calculation in (4.19), we see that the result depends only on the angle  $\alpha$  but not on  $\beta$  or  $\gamma$  in agreement with the last part of Theorem 1 and Example 7.

### 4.3. Quasi-classical limit

Faddeev's quantum dilogarithm has the following asymptotic behaviour:

$$(4.21) \quad \Phi_b\left(\frac{x}{2\pi b}\right) \Big|_{b \rightarrow 0} \sim e^{\frac{1}{2\pi i b^2} \text{Li}_2(-e^x)},$$

which implies that  $|Z_{\hbar}(X)|$  in (4.19) behaves as

$$(4.22) \quad |Z_{\hbar}(X)| \Big|_{b \rightarrow 0} \sim \left| \Phi_b\left(\frac{i(\pi - \alpha)}{2\pi b}\right) \right| \sim e^{\frac{1}{2\pi b^2} \Im \text{Li}_2(-e^{i(\pi - \alpha)})} = e^{\frac{1}{2\pi b^2} \Im \text{Li}_2(e^{-i\alpha})} = e^{-\frac{\Lambda(\alpha/2)}{\pi b^2}}.$$



Upon comparing with (3.14), the obtained formula is consistent with the following quasi-classical behaviour of the Teichmüller TQFT partition function:

$$(4.23) \quad |Z_{\hbar}(X)|_{\hbar \rightarrow 0} \sim \exp\left(-\frac{\text{vol}(X)}{2\pi\hbar}\right)$$

which is conjectured to hold for all shaped triangulations as soon as the partition function can be defined.

## References

- [1] Jørgen Ellegaard Andersen and Rinat Kashaev. A TQFT from Quantum Teichmüller Theory. *Comm. Math. Phys.*, 330(3):887–934, 2014.
- [2] Stéphane Baseilhac and Riccardo Benedetti. Quantum hyperbolic invariants of 3-manifolds with  $\text{PSL}(2, \mathbb{C})$ -characters. *Topology*, 43(6):1373–1423, 2004.
- [3] Rinat Kashaev, Feng Luo, and Grigory Vartanov. A TQFT of Turaev-Viro type on shaped triangulations. *Ann. Henri Poincaré*, 17(5):1109–1143, 2016.
- [4] Rinat M. Kashaev. On realizations of Pachner moves in 4d. *J. Knot Theory Ramifications*, 24(13):1541002, 13, 2015.
- [5] W. B. R. Lickorish. Simplicial moves on complexes and manifolds. In *Proceedings of the Kirbyfest (Berkeley, CA, 1998)*, volume 2 of *Geom. Topol. Monogr.*, pages 299–320 (electronic). Geom. Topol. Publ., Coventry, 1999.
- [6] S. V. Matveev. Transformations of special spines, and the Zeeman conjecture. *Izv. Akad. Nauk SSSR Ser. Mat.*, 51(5):1104–1116, 1119, 1987.
- [7] Sergei Matveev. *Algorithmic topology and classification of 3-manifolds*, volume 9 of *Algorithms and Computation in Mathematics*. Springer-Verlag, Berlin, 2003.
- [8] John Milnor. Hyperbolic geometry: the first 150 years. *Bull. Amer. Math. Soc. (N.S.)*, 6(1):9–24, 1982.
- [9] Udo Pachner. P.L. homeomorphic manifolds are equivalent by elementary shellings. *European J. Combin.*, 12(2):129–145, 1991.
- [10] Riccardo Piergallini. Standard moves for standard polyhedra and spines. *Rend. Circ. Mat. Palermo (2) Suppl.*, (18):391–414, 1988. Third National Conference on Topology (Italian) (Trieste, 1986).
- [11] G. Ponzano and T. Regge. Semiclassical limit of Racah coefficients. In *Spectroscopic and group theoretical methods in physics*, pages 1–58. North-Holland Publ. Co., Amsterdam, 1968.
- [12] V. G. Turaev. *Quantum invariants of knots and 3-manifolds*, volume 18 of *de Gruyter Studies in Mathematics*. Walter de Gruyter & Co., Berlin, 1994.
- [13] V. G. Turaev and O. Ya. Viro. State sum invariants of 3-manifolds and quantum 6j-symbols. *Topology*, 31(4):865–902, 1992.

Section de mathématiques, Université de Genève, 2-4 rue du Lièvre, 1211 Genève 4, Suisse, •  
rinat.kashaev@unige.ch